



# Non-volatile strain realized in the PNZST ceramics by K doping

Yangxi Yan <sup>a, \*\*</sup>, Aiyu Ding <sup>a</sup>, Zhimin Li <sup>a, \*</sup>, Maolin Zhang <sup>a</sup>, Dongyan Zhang <sup>a</sup>, Yujun Feng <sup>b</sup>, Guozhong Cao <sup>c</sup>

<sup>a</sup> School of Advanced Materials and Nanotechnology, Xidian University, Xi'an 710071, China

<sup>b</sup> Electronic Materials Research Laboratory, Key Laboratory of the Ministry of Education & International Center for Dielectric Research, Xi'an Jiaotong University, Xi'an 710049, China

<sup>c</sup> Department of Materials Science and Engineering, University of Washington, Seattle, WA 98195-2120, United States

## ARTICLE INFO

### Article history:

Received 24 September 2017

Received in revised form

19 January 2018

Accepted 21 January 2018

### Keywords:

Piezoelectrics

Doping

Defect dipole

Non-volatile strain

## ABSTRACT

The behavior of non-volatile strain was observed in K-doped  $(\text{Pb}_{0.99}\text{Nb}_{0.02})[(\text{Zr}_{0.70}\text{Sn}_{0.30})_{0.52}\text{Ti}_{0.48}]\text{O}_3$  ceramics after being poled at 180 °C. A maximum non-volatile strain of 2.6‰ was obtained in the 0.8 wt% K-doped sample and its cycling stability performed well after  $10^5$  electric cycles at 30 kV/cm. The mechanism of the defect dipole rotation was proposed to explain the large non-volatile strain. This study opens a new development window for the information storage technologies of ferroelectrics.

© 2018 Elsevier B.V. All rights reserved.

## 1. Introduction

In recent years, with the rapid development of information storage technology, the new random access memories (RAMs) with high density, high speed, non-volatile and low power consumption have been paid much attention [1,2]. To realize high speed and low power consumption, one effective way is to use the electric field to control the magnetism, instead of the magnetic field [3,4]. This can be achieved by magnetoelectric coupling effect in multiferroic materials. However, in present multiferroic materials, their magnetoelectric coefficient is too low to be employed in RAMs [5,6].

Because of the low magnetoelectric coefficient in multiferroic materials, the composite systems made of ferromagnetic and ferroelectric phases (multiferroic composite films) are explored to achieve the magnetization modulation by an electric field in RAM devices [7]. The principle of information storage in the composite films is the simultaneous strain at the ferroelectric-ferromagnetic interface. For example, when a voltage is applied across the composite structure, a strain would be generated by the ferroelectric

layer due to the piezoelectric effect, which could modify the magnetic anisotropy in the magnetic film. Thus, the magnetization state of the magnetic layer is modulated by an external electric field. However, for most of multiferroic composite films, the regulation behavior is volatile. Namely, the magnetization state will not be kept after the electric field is removed. Actually, the volatile behavior is detrimental to the information storage which requires two different states to represent the binary logical storage unit of “0” and “1”, respectively. Thus, the non-volatile behavior is necessary for multiferroic composite systems applied in the field of information storage.

The ferroelectric materials with high non-volatile strain can satisfy the requirement for information storage in multiferroic composite systems, which are characterized by two different strain states at the zero electric field, also known as the remnant strain. It had been reported that the strain level of the  $\text{Pb}(\text{Zr,Ti})\text{O}_3$  (PZT) ceramics with respect to the external driving electric field was about 0.1–0.42% [8–10], but it could not be hold after removing the driving field. Presently, the non-volatile strain in ferroelectric materials can be produced in the following cases. One is that after initially poling, the materials will have the remnant strain behavior due to the reorientation and turnover of the ferroelectric domain [11,12]. But this remnant strain is only observed in the initial measurement, and it has no substantial value. The other case is to apply an electric field with asymmetric amplitude across the

\* Corresponding author.

\*\* Corresponding author.

E-mail addresses: [xyan@xidian.edu.cn](mailto:xyan@xidian.edu.cn) (Y. Yan), [lizhmin@163.com](mailto:lizhmin@163.com) (Z. Li).

ferroelectric materials to produce the remnant strain [13,14]. However, this process requires a special electric field which restricts its practical application. The third approach is to introduce acceptors into ferroelectric materials to generate the remnant strain [15–17]. Dong et al. achieved a large remnant strain in Mn-doped  $\text{Pb}(\text{Mn}_{1/3}\text{Sb}_{2/3})\text{O}_3$ - $\text{Pb}(\text{Zr,Ti})\text{O}_3$  ceramics, and the remnant strain was quite stable after 20000 fatigue cycles [18]. Apparently, doping with appropriate acceptor is an efficient approach to achieve the non-volatile strain for the ferroelectric ceramics.

In this study, a large non-volatile strain was observed in K-doped  $(\text{Pb}_{0.99}\text{Nb}_{0.02})[(\text{Zr}_{0.70}\text{Sn}_{0.30})_{0.52}\text{Ti}_{0.48}]\text{O}_3$  (PNZST) ceramics. The stability of the strain was verified through undergoing various electric field cycles. The mechanism of the non-volatile strain arising from doping was discussed in detail.

## 2. Experimental procedures

The general formula of the studied materials was  $(\text{Pb}_{0.99}\text{Nb}_{0.02})[(\text{Zr}_{0.70}\text{Sn}_{0.30})_{0.52}\text{Ti}_{0.48}]\text{O}_3 + x \text{ wt\% K}_2\text{CO}_3$ , where  $x = 0$ –1.0. Reagent-grade oxide powders of  $\text{Pb}_3\text{O}_4$  (97.0%),  $\text{ZrO}_2$  (99.0%),  $\text{TiO}_2$  (98.0%),  $\text{SnO}_2$  (99.0%),  $\text{Nb}_2\text{O}_5$  (99.5%) and  $\text{K}_2\text{CO}_3$  (99.0%) were used as the starting materials. They were stoichiometrically weighed out and ball-milled in ethanol for 5 h. The dried mixtures were calcined at 850 °C for 2 h in air, and then pressed into the disks with 12 mm in diameter at a pressure of 200 MPa. The disks were buried in the lead oxide powder and sintered at 1300 °C for 3 h in a covered alumina crucible. The sintered pellets were polished to a thickness of 1 mm. Ag electrode paste on both sides was fired at 650 °C for 30 min. For ferroelectric characterization, electric poling was carried out at 180 °C with a 20 kV/cm DC field for 30 min. After poling, the samples were aged at room temperature for more than 15 days to establish a stable defect state.

The crystal phase structures of sintered samples were analyzed by X-ray diffraction (XRD, D8 Advance, Bruker, Germany) using  $\text{Cu K}\alpha$  radiation in the  $2\theta$  range from 15° to 70°. The surface morphologies of sintered samples were observed by scanning electron microscope (SEM, JSM-6700F, JEOL, Japan), and the compositions were analyzed by an energy-dispersive spectroscopy (EDS, NORAN System SIX Model 300, Thermo Electron Corporation, USA). The strain measurements were performed in silicon oil (temperatures ranging from 20 to 120 °C), under a triangular waveform with the

peak electric field values of  $\pm 20 \sim \pm 30$  kV/cm and at the frequency of 0.05 Hz using the aid of a Sawyer-Tower circuit (TF analyzer 2000, aixACCT, Aachen, Germany). The electric cycling experiment was conducted by a bipolar triangular electric signal with the amplitude of 30 kV/cm at 100 Hz.

## 3. Results and discussion

Fig. 1(a) shows the XRD patterns of as-prepared  $(\text{Pb}_{0.99}\text{Nb}_{0.02})[(\text{Zr}_{0.70}\text{Sn}_{0.30})_{0.52}\text{Ti}_{0.48}]\text{O}_3/x \text{ wt\% K}_2\text{CO}_3$  ceramics sintered at 1300 °C. As can be seen, all the prepared samples reveal single orthorhombic phase, and no impurity peaks are observed. The fine scan XRD patterns in the  $2\theta$  range of 37.5°–40.5° are shown in Fig. 1(b). It is found that the (111) peaks of the samples doped with K shift towards lower  $2\theta$  compared to the pure one, indicating the increase of the interplanar distance  $d$  according to the Bragg formula. The lattice constants and cell volumes of K-doped PNZST are listed in Table 1. It can be seen that the cell volume increases as the  $\text{K}_2\text{CO}_3$  amount increases from 0 wt% to 0.6 wt%. This is because that the ion radius of  $\text{K}^+$  (1.38 Å) is greater than that of  $\text{Pb}^{2+}$  (1.19 Å) at the same coordination, and in the sintering process,  $\text{K}^+$  cations occupy readily on the A sites of the crystal lattice of PNZST and substitute  $\text{Pb}^{2+}$  cations, resulting in the increase of interplanar distance and cell volume. However, when the  $\text{K}_2\text{CO}_3$  amount increases from 0.6 wt% to 1.0 wt%, the cell volume shows a slight decrease. This is possibly due to the fact that excessive  $\text{K}_2\text{CO}_3$  promotes the grain growth, which suppresses the volatilization of Pb and the formation of oxygen vacancies.

In addition, it is noted that the  $(I_{200}/I_{002})^x/(I_{200}/I_{002})^0$  and  $(I_{220}/I_{002})^x/(I_{220}/I_{002})^0$  values ( $I_{200}/I_{002}$  and  $I_{220}/I_{002}$  are the relative intensity ratios of the peak of (200) to (002) and (220) to (002), respectively, and  $x$  denotes the  $\text{K}_2\text{CO}_3$  amount and 0 denotes the undoped) initially decrease and then increase with the increasing  $\text{K}_2\text{CO}_3$  amount, as shown in Fig. 1(c). Undoubtedly, the lattice distortion is one of the important factors that affect diffraction intensity of X-ray [19]. The presence of defect dipoles ( $P_d$ ) will cause local lattice distortion and reduce the diffraction intensity of X-ray in the distorted direction [20,21]. In this study, the lattice distortion arising from defect dipoles mainly occurs in [100] and [010] directions, because the spontaneous polarization is aligned in the [110] direction. Therefore,  $I_{200}$  and  $I_{220}$  decrease more quickly than

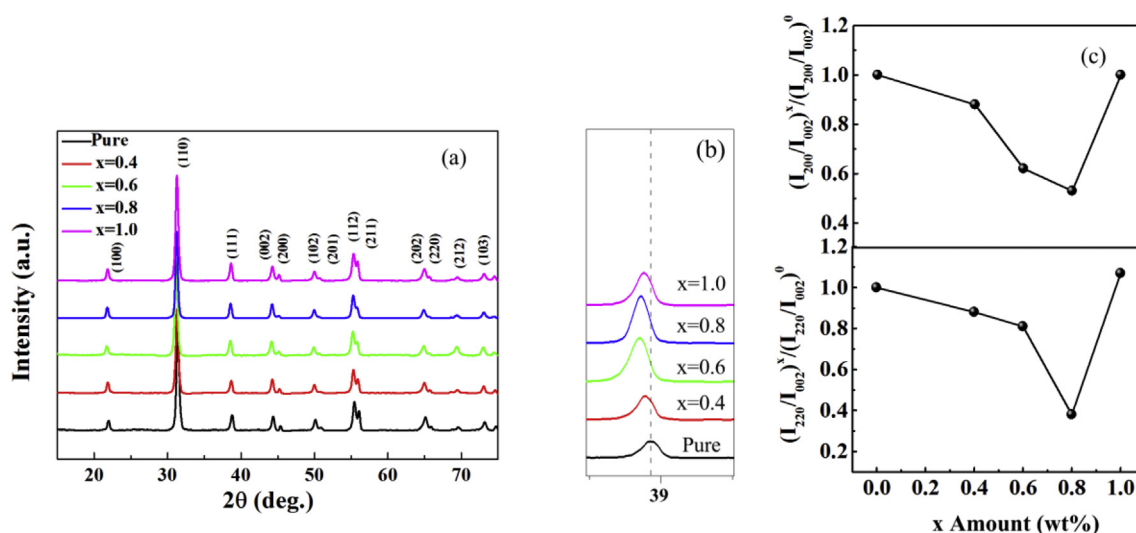


Fig. 1. (a) XRD patterns of the PNZST ceramics with different  $\text{K}_2\text{CO}_3$  amounts sintered at 1300 °C; (b) The fine scan XRD patterns in the  $2\theta$  range of 37.5°–40.5°; (c) the intensity ratios of  $(I_{200}/I_{002})^x/(I_{200}/I_{002})^0$  and  $(I_{220}/I_{002})^x/(I_{220}/I_{002})^0$ .

Download English Version:

<https://daneshyari.com/en/article/7993115>

Download Persian Version:

<https://daneshyari.com/article/7993115>

[Daneshyari.com](https://daneshyari.com)